

Quantitative Structure–Activity Relationship Studies on Hydroxamic Acids Acting as Histone Deacetylase Inhibitors

Dimitra Hadjipavlou-Litina and Eleni Pontiki

Abstract Hydroxamic acids have been found to react with both proteins and nucleic acids attracting increasing attention for their potential as highly efficacious in combating various biological targets, free radicals, and biological disorders among them cancer and inflammation. The reactivity of hydroxamic acids toward sulfhydryl groups and metal ions of proteins has been suggested to be the reason for their inhibitory effect on various enzymes. The ability of the hydroxamic acid functionality to form chelates with metals in the enzyme's active site is considered to be an important functional feature for a metalloenzyme inhibition. Many approaches in developing hydroxamic drugs, such as trichostatin and vorinostat, that interfere with (metallo) enzymes and act as anticancer drugs have been pursued over the past few decades. We present here a brief review of the QSAR and molecular modeling studies performed on hydroxamic acid derivatives acting as histone deacetylase inhibitors that have been studied as anticancer agents. These studies have shown that the anticancer activity of these compounds is basically controlled by their hydrophobic and steric properties.

Keywords Hydroxamic acids · Anticancer compounds · Quantitative structure-activity relationships · Comparative molecular field analysis · Comparative molecular similarity indices analysis · Histone deacetylase inhibitors

Abbreviations

ACxDN	Index of cohesive interactions in solids
B_1	Sterimol parameter of Verloop for the smallest width of substituent
BMLR	Best multilinear regression method
Clog P	Overall calculated lipophilicity
CMR	Molar refractivity of the whole molecule
CoMFA	Comparative molecular field analysis

D. Hadjipavlou-Litina (✉) · E. Pontiki
Department of Pharmaceutical Chemistry, School of Pharmacy, Aristotle University of
Thessaloniki, 54124 Thessaloniki, Greece
e-mail: hadjipav@pharm.auth.gr

CoMSIA	Comparative molecular similarity indices analysis
DPL	Dipole
ES-SWR	Elimination selection-stepwise regression method
FISA	Hydrophilic component of the solvent-accessible surface area
GFA	Genetic function approximation
Glob	Globularity of the compounds
HAT	Histone acetyl-transferase
HDAC	Histone deacetylase
HOMO	Highest occupied molecular orbital
L	Verloop parameter for the length of the first atom of the substituent
LFER	Linear free energy related
LSSVM	Least squares support vector machine
MgVol	MacGovan volume
MLR	Multiple linear regression
MMPs	Matrix metalloproteinases
MR _R	Molar refractivity of the substituent
MSA	Molecular shape analysis
MW	Molecular weight
PCA	Principal component analysis
PLS	Partial least squares
PMIX	Principal moment of inertia along X-axis
QSAR	Quantitative structure-activity relationships
QTMS	Quantum topological molecular similarity
r	Radius
SAR	Structure-activity relationships
SASA	Solvent-accessible surface area
ShpC	Shape coefficient
TopoJ	Balaban topological index
TSAR	Tool for structure-activity relationships
WLS	Weighted least square
WPSA	Weak polar component of the solvent-accessible surface area

Contents

1	Introduction.....	207
2	Hydroxamic Acids as Histone Deacetylase Inhibitors.....	207
	2.1 Quantitative Structure-Activity Relationships	208
	2.2 Results and Discussion	209
3	Conclusion	237
	References.....	237

1 Introduction

Hydroxamic acids constitute a chemical class sharing the same functional group in which a hydroxylamine is inserted into a carboxylic acid. Their general structure is $R-CO-NH-OH$, with a CO carbonyl group, and a hydroxylamine residue NH_2-OH . Since Lossen discovered the first of these acids more than 100 years ago, an extraordinary amount of work has been published (Murri et al. 2002; Lipczynska-Kochany 1988). In recent years, hydroxamic acid and derivatives have attracted increasing attention for their potential as highly efficacious in combating various biological targets. The chemistry and biochemistry of hydroxamic acids and their derivatives have attracted considerable attention, due to their pharmacological, toxicological, and pathological properties. Hydroxamic acids have been found to react with both proteins and nucleic acids (Niemeyer et al. 1989). The reactivity of hydroxamic acids toward sulfhydryl groups of proteins has been suggested to be the reason for their inhibitory effect on various enzymes. They are capable of the inhibition of a variety of enzymes. In terms of structure-activity relationships, hydroxamic acid moieties have been used in the design of therapeutic agents targeting cancer (Steward and Thomas 2000; Munster et al. 2001), cardiovascular diseases (Muri et al. 2002), Alzheimer's (Parvathy et al. 1998; El Yazal and Pang 2000), metal poisoning (Domingo 1998), iron-overload (Turcot et al. 2000), and as antioxidants (Green et al. 1993; Taira et al. 2002). The following is an attempt to describe in terms of (Q)SAR the role of hydroxamates as anticancer agents.

2 Hydroxamic Acids as Histone Deacetylase Inhibitors

For the last four decades, a number of potential targets have been proposed for the treatment of cancer. One of the recent targets is histone deacetylase (HDAC). Modification of histone acetylation level, promoted by histone acetyl-transferase (HAT) and HDAC enzymes, has been recognized to play an important role in the epigenetic modulation of gene expression. Histone acetyltransferases (HATs) and histone deacetylases (HDACs) are two opposing classes of enzymes, which tightly control the equilibrium of histone acetylation. Nucleosomal histone acetylation and deacetylation play an important role in the modulation of chromatin structure, chromatin function, and in the regulation of gene expression. An imbalance in the equilibrium of histone acetylation has been associated with carcinogenesis and cancer progression from rare leukemias and lymphomas to breast, prostate and ovarian cancers. The enzymatic inhibition of histone deacetylases (HDACs) has come out as a novel and efficient means for the treatment of these cancers. Inhibition of HDACs induces cell differentiation, apoptosis, and cell-cycle arrest in several cancer cell lines and in vivo preclinical models and thus HDAC inhibitors present a promising class of anticancer agents. More than 80 clinical trials are underway, testing different HDAC inhibitors in several kinds of malignant

diseases. HDAC inhibitors are able to activate differentiation, to arrest the cell cycle in G1 and/or G2, and to induce apoptosis in transformed or cancer cells. So far, a number of structurally distinct classes of compounds have been identified as HDAC inhibitors including the short-chain fatty acids, hydroxamates, cyclic tetrapeptides, and benzamides. These compounds lead to an accumulation of acetylated histone proteins both in tumor cells and in normal tissues. Several clinical trials have shown that HDAC inhibitors in well-tolerated doses have significant antitumoral activities. Half of the HDAC inhibitors under trial have the hydroxamic acid moiety, a typical zinc-binding group. One of them, SAHA, is the first HDAC inhibitor that has been approved by FDA for the second line treatment of cutaneous T cell lymphoma.

Quantitative structure-activity relationships (QSAR) studies have been reported on HDAC inhibitors in order to identify the structural determinants for anticancer activity.

2.1 Quantitative Structure-Activity Relationships

The quantitative structure-activity relationship (QSAR) studies have been of great importance in the drug design. They try to explain the observed variations in biological activities of a group of congeners in terms of molecular variations caused by a change in the substituents. Thus, they also throw the light on the mechanism of drug-receptor interactions. Among the various approaches applied to QSAR studies, the most historical and fundamental has been the parametric method developed by Hansch, which correlates the biological activity of molecules with their physicochemical, electronic, and steric properties. This parametric method by Hansch has been called as Hansch Analysis. However, it is also called the *extra thermodynamic method* or *linear free energy-related approach* as all the molecular descriptors used in this method as well as biological activity terms are linear free energy-related terms derived from rate or equilibrium constants. Besides linear free energy-related terms, this method also uses several mathematical descriptors, i.e., topological indices, such as Wiener index, Hosoya index, Randić's molecular connectivity index, and many more defined by various authors and initially used in quantitative structure-property relationship (QSPR) studies.

Apart from the Hansch approach, there have been a few more approaches, e.g., Free-Wilson, or Fujita-Ban approach, discriminated analysis, and pattern recognition technique (Gupta 2011) that have been successfully applied to QSAR studies. Additionally, there have been some manual stepwise methods, such as Topliss operation scheme, Craig plots, Fibonacci search method, and sequential simplex strategy (Siverman 2004); but these approaches have been of limited use.

All the above-mentioned QSAR approaches are related to 2-D structures of the molecules. With the advent of computer technologies came the era of 3D-QSAR studies which led to the development of methods such as distance geometry approach, comparative molecular field analysis (COMFA), comparative molecular

similarity indices analysis (COMSIA), hypothetical active site lattice (HASL) technique, *de novo* ligand design, docking (Gupta 2011), etc.

The QSAR studies on HDAC inhibitors that we are going to describe here have mostly used the 2-D Hansch approach or 3-D COMSIA or COMFA. The CoMFA calculates the steric and electrostatic interaction energies for a molecule binding with the receptor and CoMSIA is simply a modified version of CoMFA which not only calculates the steric and electrostatic interaction energies but also the hydrophobic and hydrogen-bond energies. In both the methods, the different interaction energies calculated for a series of molecules at different grid points are correlated with the biological activity using partial least square (PLS) method, also known as *projection to latent structures* technique, and are represented as 3-D contour maps in which contours of various colors represent locations on the molecular structure where low or high steric, electrostatic, hydrophobic, hydrogen-bond donor, and/or hydrogen-bond acceptor interactions would take place. A detailed discussion of these methods can be found in (Gupta 2011).

The PLS regression analysis is an alternative approach to the linear multiple regression analysis. It is used when the number of independent variables (descriptors) is relatively high compared to the number of data points (number of compounds in a given series) and several of the independent variables are mutually correlated. In such a situation, the PLS analysis generates latent variables from the linear combinations of the descriptors. These latent variables, which are orthogonal to each other, are then used to correlate the dependent variables. The quality of a PLS model can be assessed graphically by plotting the values of the dependent variable predicted by the model against the measured ones and its predictive ability is judged by calculating the cross-validated r^2 (r^2_{cv} or Q^2) (Gupta 2011).

2.2 Results and Discussion

A QSAR study was reported by Xie et al. (2004) for 124 compounds collected from various sources. A highly predictive QSAR model with $r^2 = 0.76$ and leave-one-out cross-validated $r^2 = 0.73$ was obtained. The overall rate of cross-validated correct prediction of the classification model was around 92 %. The QSAR and the classification models provided direct guidance to the internal programs for identifying and optimizing HDAC inhibitors. Limitations of the models were also discussed by the investigators.

Wang et al. (2004) developed QSAR models for a series of new trichostatin A (TSA)-like hydroxamic acids (Fig. 1) for the inhibition of cell proliferation of standard PC-3 cell line using molecular descriptors from Quikprop and electronic parameters.

The predictive ability of the proposed model was investigated using a cross-validation method. The descriptors used were: molecular weight (MW), the total solvent accessible surface area (SASA), the hydrophilic component of the solvent-accessible surface area (FISA), the weak polar component of the solvent-accessible

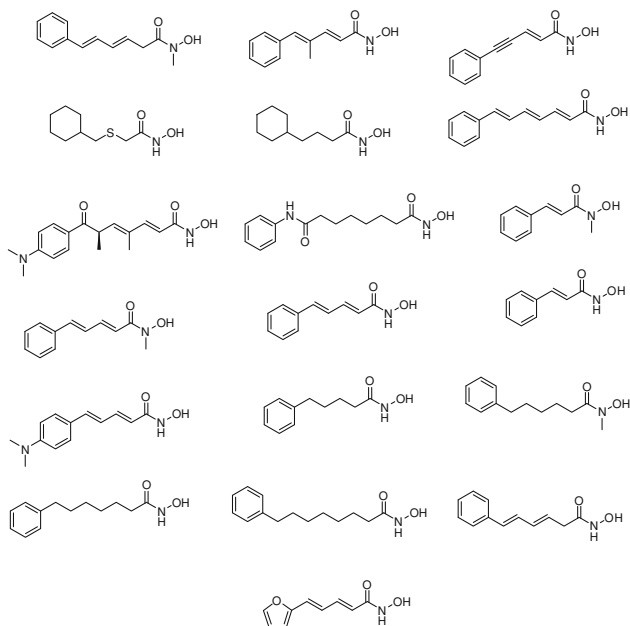


Fig. 1 Trichostatin A (TSA)-like hydroxamic acids

surface area (WPSA), an index of cohesive interactions in solids (ACxDN), the globularity of the compound (Glob) ($4\pi r^2/SASA$, whereas r is the radius of a sphere with a volume equal to the molecular volume), calculated octanol/water partition coefficient (LogP), and the PM3 atomic charge on the carbon atom of the CONHOH moiety (Qco). The derived QSAR models (Eqs. 1 and 2) reflected a PC3 cellular response driven by a net contribution of a mixture of the different HDAC enzyme in the cell as well as a contribution from the transport properties of the compounds.

$$\begin{aligned} \text{pIC}_{50}(\mu\text{M}) &= 1.96 + 14.08\text{Qco} - 15.73\text{Glob} + 0.05\text{FISA} \\ R &= 0.96, R^2 = 0.92, N = 19, F = 59.25 \\ t\text{-value: } &4.33(\text{Qco}), -4.02(\text{Glob}), 9.70(\text{FISA}) \end{aligned} \quad (1)$$

$$\begin{aligned} \text{pIC}_{50}(\mu\text{M}) &= 0.44 + 422.85\text{ACxDN} - 10.03\text{Glob} + 1.26\log P \\ R^2 &= 0.90, N = 19, F = 46.63 \\ t\text{-value: } &8.377(\text{ACxDN}), -1.551(\text{Glob}), 3.844(\log P) \end{aligned} \quad (2)$$

Equations 1 and 2 showed good linear relationship having a squared correlation coefficient R^2 of 0.96 and 0.90. Collinearity and multicollinearity tests were performed. Both models passed the collinearity test, while the second equation failed the multicollinearity test.

Park and Lee (2004) applied a computational protocol sequentially involving homology modeling, docking experiments, molecular dynamics simulation, and

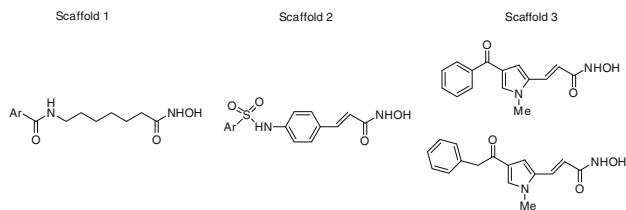


Fig. 2 Hydroxamate inhibitor scaffolds of the 12 derivatives investigated

free energy perturbation calculations in order to find the structural features of HDACIs that can increase their activity. With the newly developed force field parameters for the coordination environment of the catalytic zinc ion, FEP calculations could successfully predict the rank orders for 12 derivatives of three hydroxamate-based inhibitor scaffolds with indole amide, pyrrole, and sulfonamide moieties (Fig. 2).

The free energy of an inhibitor in aqueous solution proved to be an important factor in determining the binding free energy, showing that the increased stabilization in solution due to structural modifications must be overcome by the enzyme-inhibitor interaction. Introduction of a hydrogen-bond donor at the hydrophobic head is found to increase the inhibitory activity due to the formation of a hydrogen bond with the side chain of Asp99. Further optimization of the inhibitory potency can be achieved by elongating or enlarging the hydrophobic head so that hydrophobic interactions with Pro29 and His28, components of the flexible loop at the top of the active site, can be facilitated.

Docking simulations and 3-D quantitative structure-activity relationship (3D-QSAR) analysis were conducted by Guo et al. (2005) on a series of 29 substituted hydroxamic acid-based HDAC inhibitors with an indole amide residue at the terminus (Fig. 3) (Dai et al. 2003).

3D-QSAR models were developed using comparative molecular field analysis (CoMFA) and comparative molecular similarity indices analysis (CoMSIA). This study included two parts. The first demonstrated the common binding mode of indole amide hydroxamic acid inhibitors with HDAC, and the other derived QSAR models to find the main intermolecular interactions between inhibitors and HDAC and to predict accurately activities of newly designed inhibitors. These models could also offer valuable information about structural modification for designing new inhibitors with higher potency against HDAC.

Selected ligands were docked into the active site of human HDAC1 using the FlexX program interfaced with SYBYL 6.9. Based on the docking results, a novel

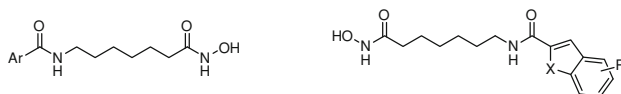


Fig. 3 Series of indole amide analogues used to obtain the models

binding mode of indole amide analogues in the human HDAC1 catalytic core was presented, and enzyme/inhibitor interactions were discussed. The indole amide group was located in the open pocket and anchored to the protein through a pair of hydrogen bonds with Asp99 O-atom and amide NH group on ligand. Based on the binding mode, predictive 3D-QSAR models were established, which had the values of conventional r^2 and cross-validated r^2 (r^2_{cv}) as 0.982 and 0.601 for CoMFA and 0.954 and 0.598 for CoMSIA, respectively.

The five similarity indices in CoMSIA (steric, electrostatic, hydrophobic, H-bond donor, and H-bond acceptor descriptors) were calculated using a C^{1+} probe atom with a radius of 1.0 Å placed at regular grid spacing of 2 Å. The derived CoMFA and CoMSIA descriptors above were used as explanatory variables, and pIC50 values were used as the target variable in PLS analysis to derive 3D-QSAR models using the implementation in the SYBYL package. The conventional correlation coefficient, r^2 , and its standard error, S , were also computed for the final PLS models. CoMFA and CoMSIA coefficient maps were generated by interpolation of the pairwise products between the PLS coefficients and the standard deviations of the corresponding CoMFA or CoMSIA descriptor values.

Both CoMFA and CoMSIA models showed similar predictive capabilities. A comparison of the 3D-QSAR field contributions with the structural features of the binding site showed good correlation between the two analyses. The results of 3D-QSAR and docking studies validated each other and provided insight into the structural requirements for activity of this class of molecules as HDAC inhibitors. The CoMFA and CoMSIA PLS contour maps and MOLCAD-generated active site electrostatic, lipophilicity, and hydrogen-bonding potential surface maps, as well as the docking studies, provided good insights into inhibitor–HDAC interactions at the molecular level.

Lu et al. (2005) provided a novel strategy of tethering short-chain fatty acids (valproate, butyrate, phenylacetate, and phenylbutyrate) with Zn^{2+} -chelating motifs through different aromatic amino acid linkers to develop a novel class of HDAC inhibitors. *N*-hydroxy-4-(4-phenylbutyryl-amino)benzamide (HTPB), a hydroxamate-tethered phenylbutyrate derivative proved to be the optimal HDACI. In this study, a structure-based optimization of HTPB was carried out using the framework generated by the crystal structure of histone deacetylase-like protein HDLP-TSA complexes.

Comparison of the HTPB docking versus TSA into the HDLP binding domain revealed unique structural features responsible for the activity. For both molecules, hydrophobic and/or π – π interactions of its scaffold with the Phe-141/Phe-198 and Tyr-91/Glu-92 subdomains play an important role in anchoring the ligand to allow optimal access of the hydroxamate group to the zinc cation. Docking studies suggested that the hydrophobic microenvironment encompassed by Phe-198 and Phe-200 could be exploited for designing more active derivatives. This premise was corroborated by the greater potency of (*S*)-(+)-*N*-hydroxy-4-(3-methyl-2-phenylbutyrylamino)-benzamide (IC₅₀ for HDAC inhibition = 16 nM) (Fig. 4), of which the isopropyl moiety was favorable for interacting with this hydrophobic

Fig. 4 (*S*)-(+)-*N*-hydroxy-4-(3-methyl-2-phenylbutyrylamino)-benzamide

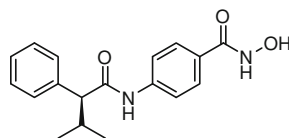
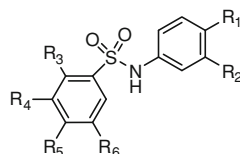


Fig. 5 Sulfonamide hydroxamic acids



motif. For the (*S*)-derivative, a high degree of flexibility was found in the active-site pocket to allow for the design of novel inhibitors with distinct stereo electronic properties.

Liu et al. (2005) obtained a CoMFA model for a series of sulfonamide hydroxamic acids HDACIs (Fig. 5). The derived model presented a good cross-validated correlation ($q^2 = 0.704$). The non-cross-validated partial least squares (PLS) model was also well built and analyzed by the prediction of the activity data by CoMFA steric, and electrostatic contours. The results showed that steric field (0.697) played a better role than the electrostatic field (0.303). Additionally, larger groups at R_5 -position and smaller groups at the R_1 -position were found to favor the activity.

Docking simulation and 3-D quantitative structure-activity relationships (3D-QSARs) analysis were conducted by Ragno et al. (2006) on a large series of compounds, including TSA, SAHA, belonging to the four different series of hydroxamic acids: TSA amide analogues (TAAs) (Jung et al. 1999), SAHA phenylalanine containing analogues (SPACAs) (Wittich et al. 2002), aroyl-pyrrolyl-hydroxy-amides (APHA1), and APHA2 (Mai et al. 2002, 2003a, b, 2004; Massa et al. 2001) (Fig. 6). The studies were performed using the GRID/GOLPE combination and led to twelve 3-D QSAR models (Tables 1 and 2) which all displayed high statistical coefficient values.

Compared to previous studies on similar inhibitors, the present 3-D QSAR investigation proved to be of higher statistical value. From the 3-D QSAR model interpretation, using the structure of a virtual HDAC 1, it was possible to depict the areas around the training set (ligand-based approach) and enzyme residues (structure-based approach), in order to have a potent HDAC inhibitor. A comparison of the 3-D QSAR maps with the structural features of the binding site showed good correlation.

In order to gain further insight into the structural requirements of HDAC inhibitors, Juvale et al. (2006) performed a 3D-QSAR study using comparative molecular field analysis (CoMFA) and comparative molecular similarity indices analysis (CoMSIA). The data set consisted of 57 hydroxamic acid analogues taken from the literature (Jung et al. 1999; Remiszewski et al. 2002; Woo et al. 2002).

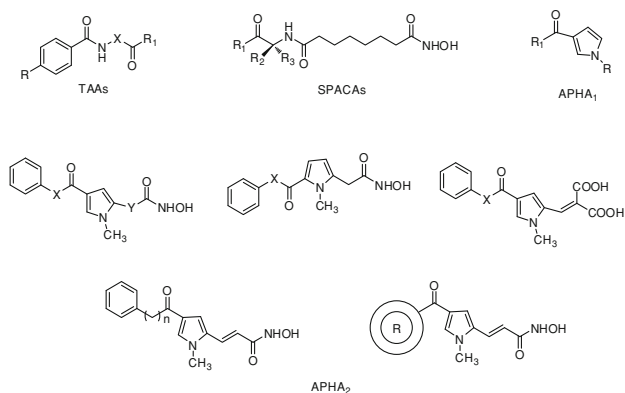


Fig. 6 HDAC inhibitors used in 3D-QSAR analysis (TAA_s TSA amide analogues, SPAC_s SAHA phenylalanine containing analogues, and APHA₁ and APHA₂ aroyl-pyrrolyl-hydroxy-amides)

Table 1 Statistical results of the 3-D QSAR models 1–8

Model	Series	Alignment	N^a	Vars ^b	PC ^c	r^2	q^2	SDEP _{CV}
1	TAA _s	TSA-based	26	622	2	0.98	0.85	0.62
2	TAA _s	SAHA-based	26	930	2	0.96	0.73	0.85
3	SPAC _s	TSA-based	21	780	3	0.98	0.72	0.29
4	SPAC _s	SAHA-based	21	805	3	0.99	0.66	0.32
5	APHA ₁	TSA-based	31	609	3	0.98	0.78	0.57
6	APHA ₁	SAHA-based	31	885	3	0.98	0.78	0.57
7	APHA ₂	TSA-based	31	745	3	0.97	0.76	0.62
8	APHA ₂	SAHA-based	31	753	2	0.95	0.78	0.62

^a Number of compounds used in the model

^b Number of selected variables

^c Number of principal components which showed the maximum q^2 value

Table 2 Statistical results of the 3-D QSAR models 9–12

Model	Series	Alignment	N^a	Vars ^b	PC ^c	r^2	q^2	SDEP _{CV}	SDEP _{test set-1}	SDEP _{test set-2}
9	United	TSA-based	103	726	3	0.90	0.75	0.69	1.20	1.46
10	United	SAHA-based	103	829	2	0.83	0.71	0.74	1.00	1.39
11	United OA ^d	TSA-based	71	659	3	0.94	0.83	0.41	1.30	1.06
12	United OA ^d	SAHA-based	71	770	3	0.91	0.75	0.51	0.96	0.99

^a Number of compounds used in the model

^b Number of selected variables

^c Number of principal components which showed the maximum q^2 value

^d OA only active compounds were used in the training set

QSAR models were derived from a training set of 40 molecules. A test set consisting of 17 molecules was used to check the external predictive ability of the CoMFA and CoMSIA models. For the superposition of the molecules on the template structure/molecule (the most active molecule) three different techniques were applied, namely RMS alignment (atom-based), multifit alignment (flexible fitting), and the SYBYL QSAR rigid body field alignment. The statistical quality of the QSAR models was assessed using the parameters r^2_{conv} , r^2_{cv} and r^2_{pred} . In addition to the steric and electronic fields, Clog *P* (calculated using ClogP/CMR application within Sybyl 6.9.1.) was also taken as a descriptor to account for lipophilicity. It has been proved that ClogP as an additional descriptor increased the statistical significance of the model, indicating that lipophilicity enhances the HDAC inhibitory activity.

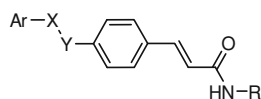
By comparing the results of the different alignments, the atom-based alignment with the hydroxamic acid functional group gave a better result than other atom-based alignment, highlighting the importance of the interaction of hydroxamic acids with the enzyme residues. Of all these alignments, the field fit alignment (along with ClogP) resulted the best in CoMFA model. The same alignment was also considered for CoMSIA where all five fields were considered in different combinations. The resulting models had good values of conventional r^2_{conv} and cross-validated r^2_{cv} -0.910 and 0.502 for CoMFA and 0.987 and 0.534 for CoMSIA, respectively.

Jaiswal et al. (2006) performed a QSAR analysis on a set of sulfonamide derivatives (Fig. 7) studied for their HDAC inhibition activity by Bouchain et al. (2003). The compounds were subjected to energy minimization and the lowest energy structure of each was used to calculate physicochemical parameters related to the thermodynamic, steric, and electronic properties of all the molecules. The best correlation revealed by a multiple regression was as shown by Eq. 3, which suggests an important role for the energy of highest occupied molecular orbital (HOMO) and torsion energy (TOE).

$$\begin{aligned} \text{pIC}_{50} &= -8.377(\pm 3.635) - 1.668(\pm 0.409)\text{HOMO} - 0.0263(\pm 0.0186)\text{TOE} \\ n &= 24, R = 0.881, \%EV = 77.6, \text{variance} = 0.138, \text{Std} = 0.372431, \\ F_{(3,20)} &= 36.369, \text{Chance} < 0.01, \text{SPRESS} = 0.422, \text{SDEP} = 0.395, \\ q^2_{\text{LOO}} &= 0.711 \end{aligned} \quad (3)$$

The HOMO descriptor bears a negative coefficient in the model, indicating that electron-withdrawing substituents will increase the affinity of sulfonamide derivatives toward histone deacetylase. Similarly, the negative coefficient of TOE

Fig. 7 General structure of sulfonamide analogues



suggests that bulky substituents are not tolerable for HDAC inhibitory activity of these compounds.

The model has a good correlation coefficient of 0.881 with 77.6 % explained variance in the HDAC inhibitory activity. *F* statistics indicated statistical significance at 99 %. Its explained variance in the activity is 77.6 % with low standard deviation value (0.37) and it has good predictive ability with $q^2_{\text{LOO}} = 0.711$ obtained by leave-one-out (LOO) method.

Wagh et al. (2006) reported a 3-D quantitative structure-activity relationship (3D-QSAR) study for a series of hydroxamic acid analogues using genetic function approximation (GFA). QSAR models were generated using a training set of 39 molecules and the predictive ability of final model was assessed using a test set of 17 molecules. The obtained QSAR model presented internal consistency of 0.712 and good external predictivity of 0.585. The results of the present QSAR study indicated that molecular shape analysis (MSA) and thermodynamic and structural descriptors are important for HDAC inhibition.

Dawson et al. (2007) conducted a QSAR analysis on the apoptotic and anti-proliferative activities of small heterodimer partner (SHP) nuclear receptor ligand, (*E*)-4-[3'-(1-adamantyl)-4'-hydroxyphenyl]-3-chlorocinnamic acid (3-Cl-AHPC), which was derived from 6-[3'-(1-adamantyl)-4'-hydroxyphenyl]-2-naphthalene-carboxylic acid (AHPN), and several carboxyl isosteric or hydrogen-bond accepting analogues. 3-Cl-AHPC continued to be the most effective apoptotic agent, whereas tetrazole, thiazolidine-2,4-dione, methylidinitrile, hydroxamic acid, boronic acid, 2-oxoaldehyde, and ethyl phosphonic acid hydrogen-bond acceptor analogues were inactive or less efficient inducers of KG-1 acute myeloid leukemia and MDA-MB-231 breast, H292 lung, and DU-145 prostate cancer cell apoptosis. Similarly, 3-Cl-AHPC was the most potent inhibitor of cell proliferation.

A fragment-based QSAR study was conducted to identify the core recognition elements of 55 analogues of AHPN and AHPC (Fig. 8) in apoptosis (MDA-MB-231). The 'overlap rule' was used to align the training set in SYBYL QSAR; and for the comparative molecular similarity index analysis (CoMSIA), electrostatic, hydrophobic, and steric fields were computed on a grid surrounding the overlapped ligands. The resulting CoMSIA analysis for apoptosis induction in MDA-MB-231 breast cancer cells resulted in a predictive R^2 of 0.78 and an un-cross-validated R^2 of 0.95 with a standard error of 0.45. It is a 3-D seven-point descriptive model with the following components: components 1 and 2, hydrogen-bond acceptor; 3, hydrogen-bond donor/acceptor; 4, hydrophobic ring; 5, hydrophobic group; 6, sterically accessible hydrophobic region; and 7, sterically accessible polar-permissible region. Key polar points include two adjacent hydrogen-bond acceptor groups and a hydrogen-bond donor/acceptor group. According to the resulting model the dimensions of the elements and their minima in computed electrostatic potential on the van der Waals surface of the fragments was found to play a major role in determining growth inhibitory activity.

Katritzky et al. (2007) tried to compare 2D- and 3D-QSAR approaches in order to correlate the inhibitory activity of a series of indole amide hydroxamic acids.

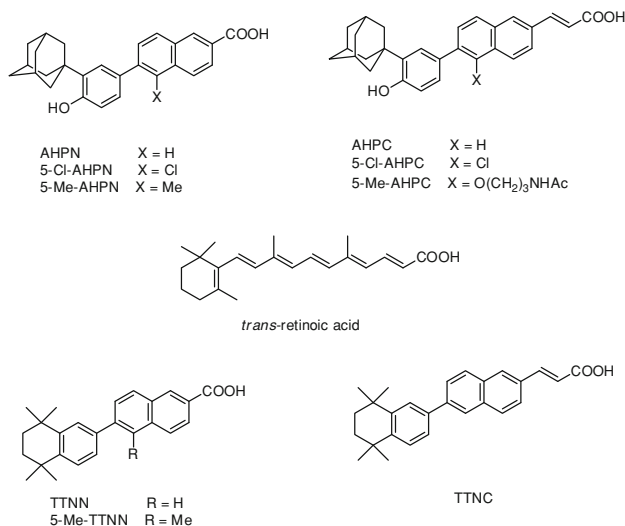


Fig. 8 Structures of some AHPN and AHPC analogues

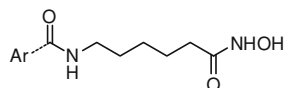
The molecules (Fig. 9) and the biological data for the study were obtained from the work of Dai et al. (2003). The study involved two alternative treatments of the activity data for the inhibition of HDACs: (i) a QSAR modeling, by multilinear regression performed by the CODESSA-PRO software which calculated about 800 different constitutional, geometrical, topological, electrostatic, quantum chemical, and thermodynamic molecular descriptors and (ii) a 3D-QSAR analysis using CoMFA method as implemented in the Chem-X software combined with a Weighted Least Squares method (WLS) for important regional mapping and docking analysis. A Partial Least Squares (PLS) procedure generated the principal components needed to build a 3D-QSAR model. All descriptors used in 2D-QSAR were derived solely from molecular structure.

A Best Multilinear Regression Method (BMLR) applied for 2D-QSR revealed the following correlation.

$$\begin{aligned}
 \log IC_{50} = & -25.31(\pm 3.20)ABOC - 9.40 \times 10^{-3}(\pm 9.98 \times 10^{-4})TMSA \\
 & + 34.59(\pm 3.67) \\
 N = & 36, R^2 = 0.778, R^2_{CVOO} = 0.721, R^2_{CVM0} = 0.721, \\
 F = & 57.71, s = 0.328
 \end{aligned}
 \tag{4}$$

In the above equation, ABOC is the average bond order for atom C and TMSA is the total molecular surface area. Molecular size and shape affect almost all

Fig. 9 General structure of amide hydroxamic acids



chemical processes. The TMSA descriptor is based on a calculation of van der Waals radii of the atoms and mainly reflects steric interactions. The ABOC descriptor defines the degree of unsaturation/aromaticity of the structure and its flexibility, which is related to the transport properties and the surface recognition profile of the molecules.

In 3D-QSAR analysis, the PLS model that used principal components exhibited the steric interactions with the following statistical parameters: $R^2 = 0.881$, predictive $R^2 = 0.708$, $Q^2 = 0.540$, predictive ERROR = 0.389. When four outliers were excluded, statistical parameters were as $R^2 = 0.937$, predictive $R^2 = 0.811$, $Q^2 = 0.624$, predictive ERROR = 0.322. The correlation coefficient of this prediction was $R^2_{\text{ext}} = 0.715$. By using the Weighted Least Square (WLS) method, R^2 maps for the steric and electrostatic fields were generated separately. The initial PLS model based on electrostatic fields had the following statistical parameters: $R^2 = 0.789$, predictive $R^2 = 0.642$, $Q^2 = 0.280$, predictive ERROR = 0.431 and after the removal of four outliers $R^2 = 0.931$, predictive $R^2 = 0.847$, $Q^2 = 0.434$, predictive ERROR = 0.295. The external predictive power of this model was evaluated and the correlation coefficient of this prediction R^2_{ext} was as 0.552. It suggests that the steric effect made a higher contribution to the biological activity than the electrostatic interaction.

Using HDAC inhibition data of Moradei et al. (2006) on some aminophenyl-benzamide and acrylamide derivatives (Fig. 10), Dessalew (2007) carried out a 2-D, 2D-QSAR study that had revealed Eq. (5), where L refers to Verloop's length parameter and B_2 and B_3 Verloop's width parameters of substituents orthogonal to length opposite to each other. This equation suggests that only the width of one side of substituents would be advantageous and the other two steric parameters will be detrimental to the activity.

$$pIC_{50} = -0.214845L + 0.452952875B_2 - 0.2152599B_3 + 2.5249031 \quad (5)$$

$$r^2 = 0.725, r^2_{\text{cv}} = .594, r^2_{\text{pred}} = 0.577$$

Ragno et al. (2008) performed molecular modeling and 3-D QSAR studies on a set of 25 aryloxopropenyl-pyrrolyl hydroxamates (Fig. 11) studied by Mai et al. (2005a, b) to gain insight into their activity and selectivity against maize HD1-B and HD1-A, the two enzymes homologous to mammalian class I and class II HDACs, respectively. The studies had been accomplished by calculating

Fig. 10 Structures of some aminophenyl-benzamides and acrylamides

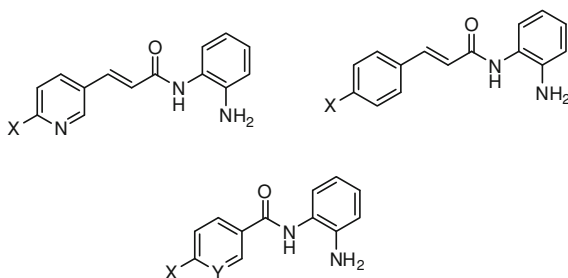
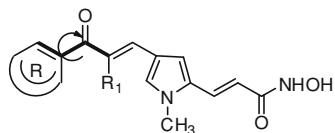


Fig. 11 Aryloxopropenyl-pyrrolyl hydroxamides

alignment-independent descriptors (GRIND descriptors) using the ALMOND software. Highly descriptive and predictive 3-D QSAR models were obtained. Comparison of the two PLS coefficient plots revealed some similarities and differences between the models. Both plots showed the distance between an H-acceptor bond group (C=O) and an aromatic portion of the cap to be the most important variable. In general, a bent molecular shape was a prerequisite for HD1-A-selective inhibitory activity, while straight shape molecular skeleton was observed to be selective to HD1-B. The reported 3-D QSAR models helped the interpretation of the selectivity issue for the class I and II HDAC inhibitors.

Chen et al. (2008a, b) built quantitative pharmacophore models from a training set of 30 diverse hydroxamic acid derivatives active as inhibitors of the HDAC1 enzyme. All pharmacophore models were generated using the Catalyst 4.10 software (Accelrys Inc., San Diego, CA) on Silicon Graphic O₂ workstation. The best pharmacophore hypothesis consisted of five pharmacophore features, including a hydrogen-bond donor, a hydrogen-bond acceptor, and three hydrophobic features. It is characterized by the highest cost difference, lower errors, lowest root mean square (rms) divergence, and best correlation coefficient of 0.924 ($r = 0.924$).

The type and spatial location of the chemical feature agree perfectly with the pattern of enzyme-inhibitor interactions (MS-275 and HDAC) identified from crystallography.

In order to investigate the potential for isoform selectivity in the inhibition of HDACs, Kozikowski et al. (2008) designed and synthesized a small series of ligands (Fig. 12) bearing the 2,4'-diaminobiphenyl scaffold in which the para-amino group bears an appendage containing either a hydroxamate or a mercaptoacetamide group coupled to an amino acid residue at the ortho-amino group. For comparison, a smaller series of substituted phenylthiazoles was also investigated by replacing the biphenyl group with a phenylthiazole containing a substituent at the 2-position or 3-position of the phenyl ring. This modification was explored based on the realization that connectivity through the five-membered thiazole ring will situate the phenyl ring substituent closer to the HDAC protein surface.

To examine the SAR of these compounds quantitatively, some QSAR equations (Eqs. 6–11) were developed against HDAC-1,2,6,8,10, where mostly two indicator variables, $I_{\text{-NHCCH}_2\text{SH}}$ and $I_{\text{-Thiazole}}$, were found

$$\begin{aligned} \text{pIC}_{50}(\text{HDAC} - 1) &= -1.844(\pm 0.248)I_{\text{-NHCCH}_2\text{SH}} + 0.983(\pm 0.149)I_{\text{-Thiazole}} \\ &\quad + 7.299(\pm 0.114) \\ n &= 23, r^2 = 0.920, \text{RMSE} = 0.322, p < 0.0001 \end{aligned} \quad (6)$$

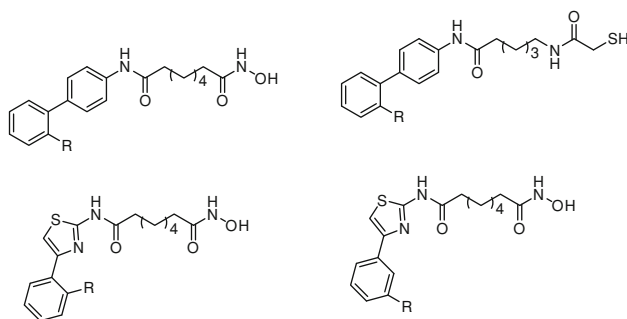


Fig. 12 General structures of biphenyl-bearing hydroxamates, mercaptoacetamides and phenylthiazole-bearing hydroxamates

$$\begin{aligned} \text{pIC}_{50}(\text{HDAC-2}) &= -1.963(\pm 0.258)I_{\text{-NHCOCH}_2\text{SH}} + 0.606(\pm 0.155)I_{\text{-Thiazole}} \\ &\quad + 6.813(\pm 0.115) \\ n &= 20, r^2 = 0.860, \text{RMSE} = 0.326, p < 0.0001 \end{aligned} \quad (7)$$

$$\begin{aligned} \text{pIC}_{50}(\text{HDAC-2}) &= -2.127(\pm 0.195)I_{\text{-NHCOCH}_2\text{SH}} \\ &\quad + 0.606(\pm 0.151)I_{\text{-Thiazole}} + 6.813(\pm 0.112) \\ n &= 22, r^2 = 0.918, \text{RMSE} = 0.318, p < 0.0001 \end{aligned} \quad (8)$$

$$\begin{aligned} \text{pIC}_{50}(\text{HDAC-6}) &= -1.429(\pm 0.246)I_{\text{-NHCOCH}_2\text{SH}} + 0.711(\pm 0.184)I_{\text{-Thiazole}} \\ &\quad + 0.046(\pm 0.023)(\text{Clog } P)^2 + 7.799(\pm 0.163) \\ n &= 23, r^2 = 0.861, \text{RMSE} = 0.384, p < 0.0001 \end{aligned} \quad (9)$$

$$\begin{aligned} \text{pIC}_{50}(\text{HDAC8}) &= -0.461(\pm 0.097)I_{\text{-NHCOCH}_2\text{SH}} + 5.668(\pm 0.040) \\ n &= 23, r^2 = 0.518, \text{RMSE} = 0.176, p < 0.0001 \end{aligned} \quad (10)$$

$$\begin{aligned} \text{pIC}_{50}(\text{HDAC-10}) &= -2.029(\pm 0.222)I_{\text{-NHCOCH}_2\text{SH}} \\ &\quad + 1.007(\pm 0.153)I_{\text{-Thiazole}} + 7.192(\pm 0.116) \\ n &= 22, r^2 = 0.916, \text{RMSE} = 0.328, p < 0.0001 \end{aligned} \quad (11)$$

to dominate. The indicator variable $I_{\text{-NHCOCH}_2\text{SH}}$ takes the value of 1.0 for the mercaptoacetamides and 0.0 for all others. The indicator variable $I_{\text{-Thiazole}}$ takes the value of 1.0 for the phenylthiazoles and 0.0 for all others. In almost all the cases mercaptoacetamides seem to be inferior to thiazoles.

Vadivelan et al. (2008) used Medichem database in order to identify HDAC inhibitors (Fig. 13). The aim of this study was: (a) to generate pharmacophore models as powerful search tools to be used as a 3-D query to identify lead molecules as HDAC inhibitors and (b) to utilize the pharmacophore model as a predictive tool for estimating biological activity of virtual molecules or molecules

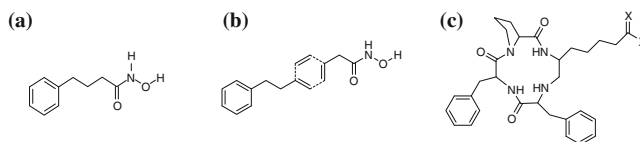


Fig. 13 Scaffolds **a**, **b**, and **c** represent three class of compounds, namely, hydroxamic acids/short-chain fatty acids, sulfa/benzamides, and cyclic tetrapeptide or epoxides, respectively

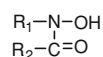
designed on the basis of structure-activity relationship analysis. A total of 20 well-defined inhibitors representing three different chemotypes were used to generate pharmacophore models using HypoGen module of catalyst. The best quantitative HypoGen model consisted of four pharmacophore features: a hydrogen-bond acceptor, a hydrophobic aliphatic feature, and two ring aromatic features, which were further validated for 378 known HDAC inhibitors with a correlation coefficient of 0.897 ($r = 0.897$). This model was further used to retrieve molecules from NCI database with 238,819 molecules. 4,638 molecules were identified as hits that satisfied the 3-D query. Among them 297 presented high, 1,433 medium, and 2,988 low activity.

A series of hydroxamic acids with the general formula $R'-C(=O)NROH$ have been designed, synthesized, and tested *in vitro* for their HDAC inhibition activity by Rajwade et al. (2008). Multivariate analytical tool, projection to latent structures was used to develop a suitably predictive model for the purpose of optimizing and identifying better HDACIs. The cross-validated Q^2_{cum} values for two optimal PLS models of hydroxamic acids were above 0.690 (remarkably higher 0.500), indicating good predictive abilities for $\log(1/IC_{50})$ values of hydroxamic acids. By partial least square regression, two QSAR models obtained revealed that, besides the essential pharmacophore $-NOHC=O$ moiety, retention capacity factor ($\log k'$), polar surface area (PSA), dipole moment (Dm), total number of hydrogen-bond donor and acceptor atoms, H, and chlorine atoms attached in upper or/and lower phenyl rings, were also important determinants for the inhibitory potency.

Continuing their research on N-aryl-substituted hydroxamic acids (Fig. 14), Rajwade et al. (2009) derived a 2D-QSAR model (Eq. 12) using principal component analysis (PCA) and partial least squares (PLS) regression.

$$\begin{aligned} \log(1/IC_{50}) &= 4.870 \times 10^{-1} \log k_w + 3.764 \times 10^{-1} I_H + 1.966 \times 10^{-1} \omega \\ &\quad - 1.646 \times 10^{-1} E_{LUMO} + 1.515 \times 10^{-1} NVE + 17.9901 \\ n &= 14, A = 1, R^2_{x(adj)(cum)} = 0.334, R^2_{y(adj)(cum)} = 0.732, Q^2_{(cum)} = 0.638, RMSEE = 0.1153, \\ &\quad RMSEP = 0.2954, \text{outliers } 5 \end{aligned} \quad (12)$$

Fig. 14 N-aryl-substituted hydroxamic acids



The model indicated that increase in lipophilicity ($\log k_w$), presence of H atom (I_H), global electrophilicity index (ω), total number of valance electrons (NVE), and decrease in energy of lowest unoccupied orbital (E_{LUMO}) value would increase the activity. The cross-validated $Q^2_{(cum)}$ values for optimal PLS model of hydroxamic acids is 0.638 (remarkably higher than 0.50), indicating good predictive ability for $\log(1/IC_{50})$ values of hydroxamic acids.

For the above case, the k-nearest neighbor molecular field analysis (kNN-MFA) was also performed. Statistically stepwise variable selection k-nearest neighbor molecular field analysis (SW-kNN-MFA) model was found comparatively better as compared to other methods. The developed SW-kNN-MFA model field plot indicated that the positive steric and electric potential were favorable for the increase in the activity and thus more bulky substituent at the 5-position of phenyl ring connected at amide group and less electronegative substituent at 3-position of phenyl ring connected to carboxyl group were postulated to be favorable for the increase in the potency of the molecules.

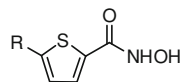
The biological data obtained by Price et al. (2007a, b) on a series of thienyl-based hydroxamic acids (Fig. 15) were analyzed by three groups of workers, Zhang et al. (2009), Pontiki and Hadjipavlou-Litina (2012), Melagraki et al. (2009). In order to rationalize the observed variance in inhibitory activity of these compounds, to propose a possible mechanism of antitumor activity and to guide the synthesis of additional compounds, Zhang et al. applied CoMFA and CoMSIA techniques. Models obtained by both the techniques exhibited the importance of steric, hydrophobic, and H-bond donor fields in the activity of the compounds.

Melagraki et al. (2009) performed a simple multiple regression analysis on a set of 58 compounds of the same series. For a training set of 45 compounds they obtained Eq. 13, in which DPL refers to the dipole moment of the compound, PMIX the principal moment of inertia along X-axis, ShpC the shape coefficient, TopoJ Balaban topological index, and ChiInf0 the Randic information index of zero order. This equation suggests that only Balaban topological index would have the favorable effect and other variables would have negative effect.

$$\begin{aligned} \log(1/IC_{50}) &= 5.69 - 0.0762 \text{ DPL} - 0.000441 \text{ PMIX} - 2.11 \text{ ShpC} \\ &\quad + 3.87 \text{ TopoJ} - 4.35 \text{ ChiInf0} \\ n &= 45, S = 0.34, R^2 = 0.78, \text{RMS} = 0.34, R^2_{\text{adj}} \\ &= 0.75, Q^2 = 0.68, \text{PRESS} = 6.59, F = 26.870 \end{aligned} \quad (13)$$

For a set of 34 compounds of the same series, Pontiki and Hadjipavlou-Litina (2012) derived the following 2D-model, exhibiting the importance of the molecular size of the compound in their HDAC inhibition activity.

Fig. 15 Structures of thienyl-based hydroxamic acids



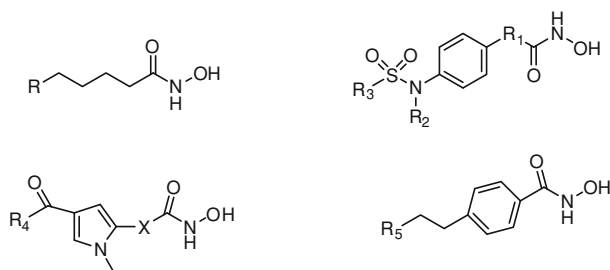


Fig. 16 Structures of hydroxamate-based HDAC inhibitors used by Chen et al

$$\begin{aligned} \log(1/IC_{50}) &= 0.012(\pm 0.002)\text{MgVol} + 3.467(\pm 0.738) \\ n &= 34, r = 0.893, r^2 = 0.797, \\ q^2 &= 0.767, s = 0.368, Q = 2.426, F_{1,32} = 125.847, \alpha = 0.01 \end{aligned} \quad (14)$$

Clog *P* vs MgVol 0.400

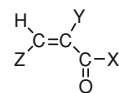
For a series of hydroxamate-based HDAC inhibitors (Fig. 16) collected from the studies of Remiszewski et al. (2002), Woo et al. (2002), Lavoie et al. (2001), Massa et al. (2001), and Delorme et al. (2001), two highly predictive and statistically significant models were derived by Chen et al. (2009) from CoMFA and CoMSIA based on pharmacophore alignment. With steric and electrostatic fields, the CoMFA model had $q^2 = 0.726$ and $r^2 = 0.998$ and with steric, electrostatic, hydrophobic, hydrogen-bond donor and acceptor fields the CoMSIA model had $q^2 = 0.610$ and $r^2 = 0.995$. Both the models were validated by an external test set, which gave a satisfactory predictive r^2 value of 0.800 and 0.732, respectively. The CoMSIA steric and electrostatic contour maps were in accordance with field distribution of CoMFA contour maps and consistent with structure-activity relationships. 3D-QSAR models seemed to agree with the active sites of HDAC as the amino acid residues interact with the three fragments of HDAC inhibitors with steric, electrostatic, hydrophobic, hydrogen bond fields around them.

Pontiki et al. (2009) tested a series of aryl-acetic and hydroxamic acids (Fig. 17) for their anticancer activity using different cancer cell lines. The activity data were subjected by us to a 2D-QSAR analysis which revealed the following correlations for different cell lines, where Eqs. 15 and 17

Human colon cancer cell lines (HT-29)

$$\begin{aligned} \log(1/IC_{50})(\text{HT} - 29) &= 0.041(\pm 0.018)\text{Esp} - \text{min} \\ &\quad + 0.093(\pm 0.039)\text{Dm} + 5.543(\pm 0.728) \\ n &= 13, r = 0.872, r^2 = 0.760, q^2 = 0.573, \\ s &= 0.078, F_{2,10} = 15.737, \alpha = 0.01 \end{aligned} \quad (15)$$

Fig. 17 Substituted aryl-acetic and hydroxamic acids



Lung cancer cells (A-549)

$$\begin{aligned} \log(1/IC_{50})(A-549) &= -0.002(\pm 0.001)\text{MgVol} \\ &\quad + 0.031(\pm 0.017)\text{Esp} - \text{min} + 5.802(\pm 0.989) \\ n &= 12, r = 0.826, r^2 = 0.683, q^2 = 0.426, \\ s &= 0.083, F_{2,9} = 9.653, \alpha = 0.01 \end{aligned} \quad (16)$$

Ovary cancer cell lines (OAW-42)

$$\begin{aligned} \log(1/IC_{50})(OAW-42) &= 0.062(\pm 0.028)\text{Esp} - \text{min} \\ &\quad + 0.084(\pm 0.065)\text{Dm} + 6.447(\pm 1.142) \\ n &= 12, r = 0.862, r^2 = 0.743, q^2 = 0.602, \\ s &= 0.128, F_{2,9} = 13.038, \alpha = 0.01 \end{aligned} \quad (17)$$

suggest that minimum electrostatic potential (Esp-min) and dipole moment (Dm) of the compounds would be crucial for their activity against colon and ovary cancer cell and lines. For lung cancer cell line, Eq. 16 however suggests that while minimum electrostatic potential may be beneficial to the activity, the molar volume may be detrimental.

The QSAR analyses did not indicate any role for lipophilicity. Electrostatic potential, dipole moments, and the bulk primarily affected the biological response.

Like above, Pontiki and Hadjipavlou-Litina (2012) reported 2-D QSAR results in a recent review on several series of hydroxamic acids acting as HDAC inhibitors as described below.

Amide Analogues of Trichostatin (Fig. 18) (Jung et al. 1999)

Lipophilicity was found to be the most significant parameter (Pontiki and Hadjipavlou 2012).

$$\begin{aligned} \log(1/IC_{50}) &= 3.716(\pm 1.742)\text{Clog } P - 2.471(\pm 1.347)(\text{Clog } P)^2 \\ &\quad + 5.702(\pm 0.404) \\ n &= 9, r = 0.925, r^2 = 0.856, q^2 = 0.713, \\ s &= 0.196, Q = 4.719, F_{2,6} = 17.792, \\ \alpha &= 0.01, \text{Clog } P_o = 0.752(\pm 0.129) \text{ from } 0.674 \text{ to } 0.931 \end{aligned} \quad (18)$$

Sulfonamide hydroxamic acids (Lavoie et al. 2001) (Fig. 19)

Fig. 18 Hydroxamates synthesized by Jung et al.

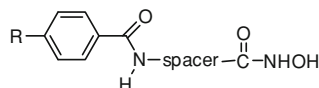
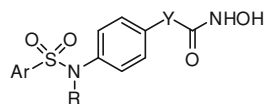


Fig. 19 Sulfonamide synthesized by Lavoie et al.



a.

$$\begin{aligned} \log(1/IC_{50})(\text{recombinant human HDAC} - 1) &= -0.240(\pm 0.189)CMR \\ &+ 1.444(\pm 0.463)I_{-CH=CH} \\ &- 1.059(\pm 0.658)\sigma_p + 7.727(\pm 1.629) \\ n &= 18, r = 0.882, r^2 = 0.779, \\ q^2 &= 0.666, s = 0.331, Q = 2.665, \\ F_{3,14} &= 16.421, \alpha = 0.01, \\ \text{Clog } P \text{ vs CMR} &= 0.579 \end{aligned} \quad (19)$$

CMR represents the molar refractivity of the molecules. Its negative sign brings out a steric effect. The presence of a double bond seems to be favorable for the inhibitory activity. The role of σ_p (Hammett) term of *p*-substituents of R was found to be important.

b. The *in vitro* antiproliferative activity at human colon cancer HCT 116 cells

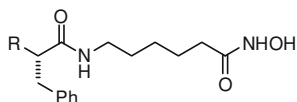
$$\begin{aligned} \log(1/EC_{50}) &= -0.282(\pm 0.164)CMR + 1.406(\pm 0.388)I_{-CH=CH} \\ &- 1.247(\pm 0.627)\sigma_p + 7.397(\pm 1.44) \\ n &= 17, r = 0.916, r^2 = 0.840, q^2 = 0.747, s = 0.290, Q = 3.159, \\ F_{3,13} &= 22.733, \alpha = 0.01, \text{Clog } P \text{ vs CMR} = 0.571 \end{aligned} \quad (20)$$

CMR, $I_{-CH=CH}$ and σ_p were found to be conducive in this case also

c. T24 cancer cells

$$\begin{aligned} \log(1/EC_{50}) &= -0.356(\pm 0.220)\text{Clog } P \\ &+ 0.428(\pm 0.178)L_4 + 4.723(\pm 0.479) \\ n &= 11, r = 0.893, r^2 = 0.797, q^2 = 0.725, \\ s &= 0.199, Q = 4.487, \\ F_{2,8} &= 15.697, \alpha = 0.01, \text{Clog } P \text{ vs } L_4 = 0.207 \end{aligned} \quad (21)$$

Fig. 20 Succinimide hydroxamic acids synthesized by Curtin et al.



Hydrophilicity with a negative sign of Clog P seemed to be important followed by the Verloop parameter (L_4) for the length of the first atom of the substituent at the 4-position of the phenyl ring.

Succinimide Hydroxamic acids (Curtin et al. 2002) (Fig. 20)

For the antiproliferative activity in human HT1080 fibrosarcoma cells of these compounds the equation obtained was as

$$\begin{aligned} \log(1/IC_{50}) &= 0.379(\pm 0.316)MR_R + 4.070(\pm 1.500) \\ n &= 5, r = 0.911, r^2 = 0.829, q^2 = 0.567, s = 0.293, Q = 3.109, \\ F_{1,3} &= 14.568, \alpha = 0.01, \text{Clog } P \text{ vs } MR_{-R} = 0.436 \end{aligned} \quad (22)$$

Simple Trichostatin A-Like Straight Chain Hydroxamates (Woo et al. 2002) (Fig. 21)

$$\begin{aligned} \log(1/IC_{50}) &= 2.099(\pm 1.027)CMR - 0.094(\pm 0.059)CMR^2 - 3.238(\pm 4.420) \\ n &= 23, r = 0.909, r^2 = 0.826, q^2 = 0.777, s = 0.332, \\ Q &= 2.738, F_{2,20} = 47.435, \alpha = 0.01, \\ CMR_0 &= 11.157(\pm 2.576) \text{ from } 10.122 \text{ to } 15.274 \end{aligned} \quad (23)$$

Molar refractivity of the whole molecule is found to be the most important variable. CMR in a parabolic model explains 82.6 % of the variance.

Phenylalanine Containing Inhibitors of Histone Deacetylase (Wittich et al. 2002) (Fig. 22)

a. Maize HD inhibition

$$\begin{aligned} \log(1/IC_{50}) &= 0.359(\pm 0.154)\text{Clog } P + 0.141(\pm 0.089)MR_{R'} + 5.953(\pm 0.267) \\ n &= 16, r = 0.892, r^2 = 0.796, q^2 = 0.713, s = 0.236, Q = 3.780, \\ F_{2,13} &= 25.356, \alpha = 0.01, \text{Clog } P \text{ vs } MR_{-R'} = 0.080 \end{aligned} \quad (24)$$

Fig. 21 TSA like straight chain hydroxamate analogues

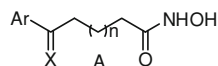
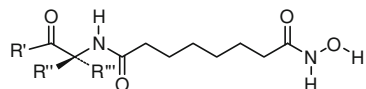


Fig. 22 Phenylalanine containing inhibitors of histone deacetylase



b. Proliferation of the Friend leukemic cells

$$\begin{aligned} \log(1/IC_{50}) &= 0.543(\pm 0.197)C\log P - 0.413(\pm 0.125)MR_{R'} + 5.010(\pm 0.225) \\ n &= 15, r = 0.905, r^2 = 0.818, q^2 = 0.739, s = 0.251, Q = 3.606, \\ F_{2,12} &= 27.044, \alpha = 0.01, C\log P \text{ vs } MR_{R'} 0.470 \end{aligned} \quad (25)$$

In both the above cases the hydrophobicity of the molecule is found to have a positive effect, while the molar refractivity of R'' -substituent has the positive effect for maize HD-2 inhibition and that of R' -substituent a negative effect in proliferation of the Friend leukemic cells.

Indole Amide Hydroxamic Acids (Dai et al. 2003) (Fig. 23)

a. HDAC-1 and HDAC-2 Inhibition

$$\begin{aligned} \log(1/IC_{50}) &= 0.167(\pm 0.108)MR_{Ar} + 1.892(\pm 0.481)I_{IND} \\ &+ 0.507(\pm 0.227)I_2 + 4.894(\pm 0.619) \\ n &= 32, r = 0.881, r^2 = 0.776, q^2 = 0.709, s = 0.303, Q = 2.908, \\ F_{3,28} &= 32.257, \alpha = 0.01, C\log P \text{ vs } MR_{AR} 0.784 \end{aligned} \quad (26)$$

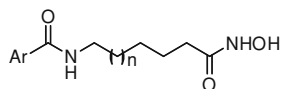
This equation suggests a favorable role for molar refractivity of aromatic group Ar and an additional positive effect if Ar is an indolyl group since an indicator parameter I_{IND} used for it is positive. I_2 is an additional indicator variable used for a substituent at the 2-position of Ar group. The positive coefficient of it suggests a positive effect of such a substituent.

b. Antiproliferative activity against human HT1080 fibrosarcoma cell line

$$\begin{aligned} \log(1/IC_{50}) &= -0.007(\pm 0.004)MgVol + 0.654(\pm 0.491)MR_4 + 8.699(\pm 1.415) \\ n &= 12, r = 0.852, r^2 = 0.725, q^2 = 0.575, s = 0.192, Q = 4.438, \\ F_{2,9} &= 11.89, \alpha = 0.01, MR_4 \text{ vs } C\log P 0.107 \end{aligned} \quad (27)$$

MgVol (molar volume) with a negative sign is shown to have an unfavorable steric effect, but the MR_4 , the molar refractivity of the substituent at the 4-position of aryl moiety, is shown to have the positive effect.

Fig. 23 Indole amide hydroxamic acids



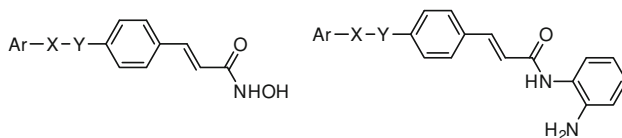


Fig. 24 Sulfonamide analogues

Sulfonamide Derivatives (Bouchain et al. 2003) (Fig. 24).

The inhibitory activity of these compounds on partially purified recombinant human HDAC-1 was shown to be with molar refractivity as shown by Eq. 28, where the molar refractivity of the whole molecule was shown detrimental to the activity but that of only aromatic group to be favorable. The whole molecule may create the steric problem but the aromatic group might be involved in a dispersion interaction with some site of the receptor.

$$\begin{aligned} \log(1/IC_{50}) &= -0.455(\pm 0.104)CMR \\ &\quad + 0.506(\pm 0.190)MR_{Ar} + 9.537(\pm 1.022) \\ n &= 27, r = 0.879, r^2 = 0.772, q^2 = 0.708, \\ s &= 0.374, Q = 2.350, F_{2,24} = 40.716, \alpha = 0.01 \end{aligned} \quad (28)$$

N-Hydroxy-3-phenyl-2-propenamides (Remiszewski et al. 2003) (Fig. 25).

The activity of these compounds against HCT116 human colon carcinoma cells was found to be correlated with molar refractivity as shown by Eq. 29, where MR_{R_1} refers to the molar refractivity of only R_1 -substituent. This equation suggests that only the molecular size of the R_1 -substituent is important for the activity but a larger size ($MR_{R_1} > 4.714$) will be detrimental to the activity, which may be probably due to steric effect.

$$\begin{aligned} \log(1/IC_{50}) &= 27.613(\pm 25.161)MR_{R_1} \\ &\quad - 2.929(\pm 2.826)(MR_{R_1})^2 - 57.237(\pm 55.740) \\ n &= 10, r = 0.862, r^2 = 0.744, \\ q^2 &= 0.566, s = 0.430, Q = 2.005, \\ F_{2,7} &= 10.151, \alpha = 0.01, (MR_{R_1})_0 = 4.714(\pm 3.797) \text{ from } 4.530 \text{ to } 12.124 \end{aligned} \quad (29)$$

(Aryloxopropenyl)pyrrolyl Hydroxyamides (Mai et al. 2003a) (Fig. 26).

The activity of this series of compounds tested against the HD1-A was also shown to correlate with molecular refractivity as shown by Eq. 30. However, this

Fig. 25 *N*-Hydroxy-3-phenyl-2-propenamides

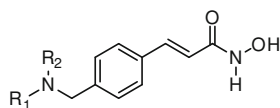
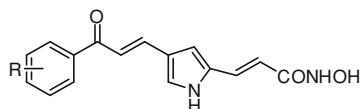
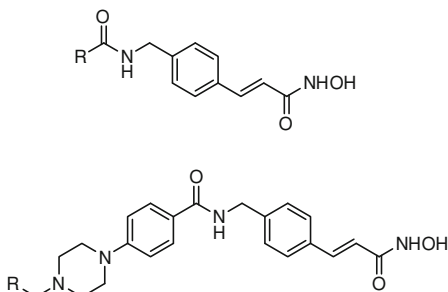


Fig. 26 (Aryloxopropenyl) pyrrolyl hydroxyamides**Fig. 27** 3-(4-Substituted-phenyl)-*N*-hydroxy-2-propenamides

equation exhibited that the molecular refractivity of only R-substituent at 2-position of the phenyl ring was effective.

$$\begin{aligned} \log(1/IC_{50}) &= 1.534(\pm 0.890)MR_{R2} + 6.366(\pm 0.309) \\ n &= 6, r = 0.923, r^2 = 0.851, \\ q^2 &= 0.735, s = 0.178, Q = 5.185, F_{1,4} = 23.484, \alpha = 0.01 \end{aligned} \quad (30)$$

3-(4-Substituted-phenyl)-N-hydroxy-2-propenamides (Kim et al. 2003) (Fig. 27).

For this series of compounds, their antiproliferative activity was reported against human lung cancer-A549 cell lines as well as human cell lines of breast cancer (SK-BR-3). Both the activities were shown to be significantly correlated with ClogP as exhibited by Eqs. 31 and 32, respectively, suggesting that hydrophilicity of these compounds was the major controlling factor of their activity

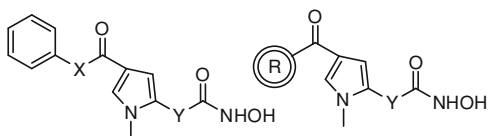
$$\begin{aligned} \log(1/IC_{50}) &= 0.755(\pm 0.265)Clog P + 4.984(\pm 0.338) \\ n &= 6, r = 0.970, r^2 = 0.940, q^2 = 0.892, \\ s &= 0.112, Q = 8.661, F_{1,4} = 62.560, \alpha = 0.01 \end{aligned} \quad (31)$$

$$\begin{aligned} \log(1/IC_{50}) &= 1.058(\pm 0.514)Clog P + 4.909(\pm 0.657) \\ n &= 6, r = 0.944, r^2 = 0.891, q^2 = 0.778, \\ s &= 0.217, Q = 4.350, F_{1,4} = 32.638, \alpha = 0.01 \end{aligned} \quad (32)$$

3-(4-Aroyl-1-methyl-1H-2-pyrrolyl)-N-hydroxy-2-propenamides (Mai et al. 2004) (Fig. 28).

For the inhibitory data of these compounds on maize histone deacetylase HD-2, a bilinear model, as shown by shown by Eq. 33, was reported.

Fig. 28 3-(4-Aroyl-1-methyl-1*H*-2-pyrrolyl)-*N*-hydroxy-2-propenamides



$$\begin{aligned} \log(1/IC_{50}) &= 1.804(\pm 0.707)CMR - 2.193(\pm 0.957)\log(\beta \cdot 10^{CMR} + 1) \\ &\quad + 1.074(\pm 0.353)I_{CH=CH} - 8.583(\pm 5.442) \\ n &= 22, r = 0.931, r^2 = 0.868, q^2 = 0.773, s = 0.358, Q = 2.601, \\ F_{4,17} &= 27.856, \alpha = 0.01, (CMR)_0 = 8.953, \log \beta: -8.286 \end{aligned}$$

$$\text{Clog } P \text{ vs } CMR = 0.835 \quad (33)$$

This equation suggests that instead of a parabola, the correlation had a Λ -shaped curve. Whatsoever, the correlation indicated a positive role of molar refractivity of the compound till CMR attains an optimum value equal to 8.953. Indicator variable $I_{CH=CH}$ was used for analogues where X or Y bridge could be $-CH=CH-$. Its positive coefficient indicates that these compounds might be more active.

Pthalimide-type HDACIs (Shinji et al. 2005) (Fig. 29).

For this series of compounds also, the molar refractivity was found to play an important role as shown by Eq. 34. As is obvious, this equation suggests that while molar refractivity of R-substituent may be detrimental to the activity that of R_1 group would be conducive. The R-substituent might produce the steric effect, while R_1 group may participate in dispersion interaction with the receptor.

$$\begin{aligned} \log(1/EC_{50}) &= -0.337(\pm 0.153)MR_R \\ &\quad + 1.376(\pm 0.589)MR_{R_1} + 4.871(\pm 1.129) \\ n &= 13, r = 0.892, r^2 = 0.795, q^2 = 0.638, \\ s &= 0.318, Q = 2.805, F_{2,10} = 19.405, \alpha = 0.01 \end{aligned} \quad (34)$$

Cyclic amide/imide-bearing hydroxamic acid derivatives (Shinji et al. 2006) (Fig. 30).

For this series of compounds the HDAC-6 inhibitory activity was found to correlate with ClogP and Taft's steric factor as shown by Eq.35, which suggests that not the hydrophobic but the hydrophilic property of the molecule would be

Fig. 29 Pthalimide-type HDACIs

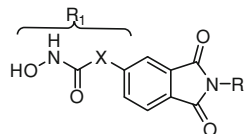
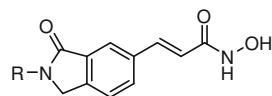


Fig. 30 Cyclic amide/imide-bearing hydroxamic acid derivatives



conductive and some steric interaction of 3-substituent in R-moiety may also be beneficial.

$$\begin{aligned} \log(1/IC_{50}) &= -0.199(\pm 0.086)Clog P - 0.101(\pm 0.093)E_{S-3} \\ &\quad + 6.775(\pm 0.196) \\ n &= 16, r = 0.835, r^2 = 0.698, q^2 = 0.571, s = 0.115, Q = 7.261, \\ F_{2,13} &= 15.053, \alpha = 0.01, Clog P \text{ vs } E_{S-3} 0.000 \end{aligned} \quad (35)$$

Novel uracil-based hydroxamates (Mai et al. 2005a, b) (Fig. 31).

The synthesized compounds were tested in different forms of HDAC.

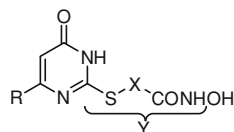
For uracil-based hydroxamates reported by Mai et al. (Mai et al. 2005a, b) (Fig. 31), their maize HDAC class II (HD1-A) inhibition activity was found to be correlated as shown by Eq. 36 and maize HDAC class I (HD1-B) inhibition activity as shown by Eq. 37. Both the equations are parallel and suggest that both the activities would depend on the molar refractivity of Y moiety of the compounds with almost an equal optimum value of MR_Y around 4.5. This Y moiety may be assumed to have dispersion interaction with the receptor.

$$\begin{aligned} \log(1/IC_{50}) &= 8.498(\pm 4.610)MR_Y - 0.934(\pm 0.578)(MR_Y)^2 - 11.843(\pm 9.090) \\ n &= 11, r = 0.919, r^2 = 0.844, q^2 = 0.781, \\ s &= 0.389, Q = 2.362, F_{2,8} = 21.704, \alpha = 0.01, \\ (MR_Y)_o &= 4.548(\pm 0.662) \text{ from } 4.246 \text{ to } 5.571 \end{aligned} \quad (36)$$

$$\begin{aligned} \log(1/IC_{50}) &= 8.621(\pm 4.124)MR_Y - 0.998(\pm 0.517)(MR_Y)^2 \\ &\quad - 11.268(\pm 8.122) \\ n &= 10, r = 0.917, r^2 = 0.842, q^2 = 0.668, \\ s &= 0.332, Q = 2.762, F_{2,7} = 18.588, \alpha = 0.01, (MR_Y)_o \\ &= 4.317(\pm 0.340) \text{ from } 4.104 \text{ to } 4.784 \end{aligned} \quad (37)$$

Pyrimidyl-5-Hydroxamic Acids (Angibaud et al. 2005) (Fig. 32).

Fig. 31 Novel uracil-based hydroxamates



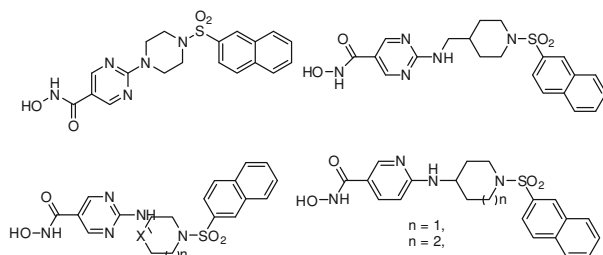


Fig. 32 Pyrimidyl-5-hydroxamic acids

The above compounds were tested on HeLa cell nuclear extracts as a source of HDAC enzyme. For these data the following 2D-QSAR model was formulated suggesting that bulky molecule will not be favorable to the activity.

$$\begin{aligned} \log(1/IC_{50}) &= -0.030(\pm 0.014)MgVol + 20.759(\pm 6.169) \\ n &= 8, r = 0.908, r^2 = 0.824, q^2 = 0.718, s = 0.161, Q = 5.640, \\ F_{1,6} &= 27.646, \alpha = 0.01 \end{aligned} \quad (38)$$

(Aryloxopropenyl)pyrrolyl Hydroxamides (Mai et al. 2005a) (Fig. 33).

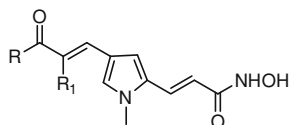
These compounds were tested against maize HDACs (HD1-B and HD1-A).

For maize HD-1-A inhibition activity of this series of compounds the correlation obtained was as

$$\begin{aligned} \log(1/IC_{50}) &= -0.025(\pm 0.008)MgVol + 1.813(\pm 0.826)B_{1-2} \\ &+ 12.524(\pm 2.688) \\ n &= 18, r = 0.893, r^2 = 0.798, q^2 = 0.693, s = 0.418, Q = 2.136, \\ F_{2,15} &= 59.114, \alpha = 0.01, MgVol \text{ vs } B_{1-2} = 0.020 \end{aligned} \quad (39)$$

which revealed the role of steric effects. This coincides with the molecular modeling results of Mai et al. (2005b) which had pointed out that a bent molecular shape structure was a prerequisite for HD1-A-selective inhibitory activity. MacGowan volume (MgVol) with negative sign implies steric hindrance. B_{1-2} is the sterimol parameter of Verloop for the smallest width of substituent at the 2-position of the phenyl ring at R. It seems that as the smallest width of substituent increases, the inhibitory activity also increases.

Fig. 33 (Aryloxopropenyl) pyrrolyl hydroxamides



For the maize HD1-B inhibitory activity of these compounds the correlation obtained was as

$$\begin{aligned} \log(1/IC_{50}) &= -1.747(\pm 0.933)\text{Clog } P + 0.889(\pm 0.491)L_{-2} + 6.275(\pm 2.091) \\ n &= 18, r = 0.836, r^2 = 0.699, q^2 = 0.560, \\ s &= 0.631, Q = 1.325, F_{2,15} = 17.365, \\ \alpha &= 0.01, \text{Clog } P \text{ vs } L_{-2} = 0.013 \end{aligned} \quad (40)$$

where negative Clog P term indicates that hydrophilic molecules would present better inhibitory activity. L_{-2} , the sterimol parameter for the length of the substituent at the 2-position of the aryl ring R would influence the activity positively.

Rigid Trichostatin A analogues (Charrier et al. 2006) (Fig. 34).

These trichostatin analogues were tested for their antiproliferative activity against non-small cell lung cancer H661 cells and their activity was found to be significantly correlated with hydrophobicity as

$$\begin{aligned} \log(1/IC_{50}) &= -0.343(\pm 0.242)\text{C log } P + 6.382(\pm 0.627) \\ n &= 6, r = 0.891, r^2 = 0.795, q^2 = 0.567, s = 0.134, Q = 6.649, \\ F_{1,4} &= 15.389, \alpha = 0.05 \end{aligned} \quad (41)$$

which suggest that not the hydrophobicity but hydrophilicity of the compounds would be important for their activity.

Hydrophilic Hydroxamates and 2-aminobenzamide-containing derivatives (Nagaoka et al. 2006) (Fig. 35).

These compounds were tested for their HDAC inhibitory activity and HCT116 colon carcinoma cell antiproliferative activity. For both these activities the correlations obtained were as shown by Eqs. 42 and 43, which suggests that both the activities will be primarily governed by hydrophobic property of the molecule. Thus the whole molecule in both the cases might be involved in hydrophobic interaction with the receptors. In Eq. 42, the presence of an indicator variable used for R=OH, however, indicates that HDAC inhibition activity may have an additional advantage of the presence of an OH moiety at R, and this may be due to the participation of OH in hydrogen bonding with some site of the receptor.

Fig. 34 TSA analogues

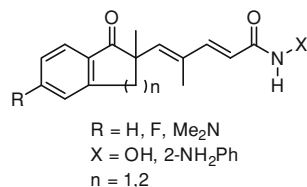
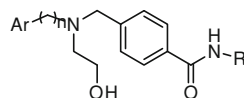


Fig. 35 Hydrophilic Hydroxamates and 2-aminobenzamide-containing derivatives



$$\begin{aligned} \log(1/IC_{50}) &= 0.387(\pm 0.358)\text{Clog } P \\ &\quad + 1.873(\pm 0.668)I_{OH} + 4.626(\pm 0.908) \\ n &= 10, r = 0.933, r^2 = 0.871, q^2 = 0.761, \\ s &= 0.355, Q = 2.628, F_{2,7} = 23.683, \\ \alpha &= 0.01, \text{Clog } P \text{ vs } I_{OH} = 0.243 \end{aligned} \quad (42)$$

$$\begin{aligned} \log(1/IC_{50}) &= 0.434(\pm 0.175)\text{Clog } P + 4.207(\pm 0.357) \\ n &= 9, r = 0.911, r^2 = 0.831, q^2 = 0.737, s = 0.217, Q = 4.198, \\ F_{1,7} &= 34.427, \alpha = 0.01 \end{aligned} \quad (43)$$

SAHA analogues functionalized adjacent to the hydroxamic acid (Bieliauskas et al. 2007) (Fig. 36).

For a small series of SAHA analogues, the correlation obtained was as

$$\begin{aligned} \log(1/IC_{50}) &= 0.389(\pm 0.283)B_{5-R} + 2.316(\pm 1.099) \\ n &= 6, r = 0.886, r^2 = 0.784, q^2 = 0.505, s = 0.149, Q = 5.946, \\ F_{1,4} &= 14.651, \alpha = 0.05 \end{aligned} \quad (44)$$

where B_{5-R} is the Sterimol parameter of Verloop for the largest width of R-substituent. The positive coefficient of B_{5-R} suggests that this substituent might be involved in some dispersion interaction with the receptor.

Aminosuberoyl hydroxamic acids (Belvedere et al. 2007) (Fig. 37).

The aminosuberoyl hydroxamic acids were tested for their activity against HDAC-1 for which the correlation obtained was as

$$\begin{aligned} \log(1/IC_{50}) &= -12.545(\pm 4.636)MR_{R_1} + 1.934(\pm 0.686)(MR_{R_1})^2 \\ &\quad + 27.415(\pm 7.566) \\ n &= 14, r = 0.924, r^2 = 0.854, q^2 = 0.778, \\ s &= 0.236, Q = 3.915, F_{2,11} = 32.184, \\ \alpha &= 0.01, (MR_{R_1})_0 = 3.244(\pm 0.080) \text{ from } 3.145 \text{ to } 3.305 \end{aligned} \quad (45)$$

Fig. 36 SAHA analogues functionalized adjacent to the hydroxamic acid

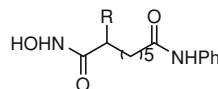
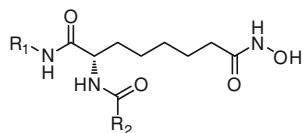


Fig. 37 Aminosuberoyl hydroxamic acids

which suggests that the molar refractivity of R_1 -substituent would govern the activity but would have the positive effect only after MR_{R_1} attains an optimum value of 3.244. An R_1 -substituent of larger size might be involved in dispersion interaction.

δ-Lactam-Based Histone Deacetylase Inhibitors 9 (Fig. 38) (Kim et al. 2007).

For the HDAC inhibitory enzyme activities of these compounds obtained from HeLa cell lysate the following model was derived by Pontiki and Hadjipavlou (2012) to suggest that lipophilicity is the most important parameter describing the activity of these compounds.

$$\begin{aligned} \log(1/IC_{50}) &= 0.556(\pm 0.360)\text{Clog } P + 5.870(\pm 0.389) \\ \log(1/IC_{50}) &= 0.556(\pm 0.360)\text{Clog } P + 5.870(\pm 0.389) \\ n &= 6, r = 0.906, r^2 = 0.821, q^2 = 0.506, s = 0.243, Q = 3.728, \\ F_{1,4} &= 18.295, \alpha = 0.05 \end{aligned} \quad (46)$$

2-Aroyloindoles and 2-Aroylbenzofurans with N-Hydroxyacrylamide Substructures (Mahboobi et al. 2007) (Fig. 39).

E-N-hydroxy-(2-aryloindole)acrylamides and *E-N*-hydroxy-(2-arylbzofuran)acrylamides were profiled using nuclear extra HDAC and recombinant HDAC-1. For HDAC inhibitory activity the correlation obtained was as shown by Eq. 47 and HDAC-1 inhibitory activity the correlation obtained was as shown by Eq. 48. As is obvious, while the molar refractivity of R_2 -substituent at the 3-position of the phenyl ring will favor the HDAC inhibitory after it attains an optimum value equal to 0.707, the molar refractivity of R_2 -substituent at the 4-position of the phenyl ring and that of R_3 group would be detrimental to HDAC-1 inhibitory activity.

$$\begin{aligned} \log(1/IC_{50}) &= -0.875(\pm 0.677)MR_{R_{2-3}} + 0.618(\pm 0.307)(MR_{R_{2-3}})^2 \\ &\quad + 6.528(\pm 0.196) \\ n &= 13, r = 0.936, r^2 = 0.876, q^2 = 0.784, \\ s &= 0.184, Q = 5.086, F_{2,13} = 35.294, \\ \alpha &= 0.01, (MR_{R_{2-3}})_o = 0.707(\pm 0.287) \text{ from } 0.308 \text{ to } 0.864 \end{aligned} \quad (47)$$

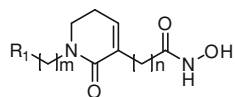
Fig. 38 *δ*-Lactam-based histone deacetylase inhibitors

Fig. 39 2-Aroyloindoles and 2-arylbenzofurans with *N*-hydroxyacrylamide substructures

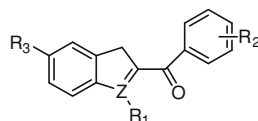


Fig. 40 Triazolylphenyl derivatives



$$\begin{aligned} \log(1/IC_{50}) &= -0.418(\pm 0.162)MR_{R3} - 0.514(\pm 0.172)MR_{R2-4} \\ &\quad + 7.388(\pm 0.295) \\ n &= 13, r = 0.916, r^2 = 0.839, q^2 = 0.737, s = 0.215, Q = 4.260, \\ F_{2,13} &= 25.995, \alpha = 0.01 \end{aligned} \quad (48)$$

Triazolylphenyl-Based Histone Deacetylases Inhibitors (Chen et al. 2008b) (Fig. 40).

For this series of compounds, their activity against HDAC-1 and HDAC-3 was found to correlate with MR_{-3Ph} , the molar refractivity of substitution at 3-position of the phenyl group (X), and $ClogP$ as shown by Eqs. 49 and 50, respectively. The hydrophobicity is shown to have the effect only on HDAC-1 inhibitory activity and not on that of HDAC-3.

$$\begin{aligned} \log(1/IC_{50}) &= 0.157(\pm 0.153) Clog P + 0.137(\pm 0.031)MR_{-3Ph} \\ &\quad + 6.741(\pm 0.381) \\ n &= 15, r = 0.949, r^2 = 0.900, q^2 = 0.839, \\ s &= 0.108, Q = 8.787, F_{2,12} = 54.170, \\ \alpha &= 0.01, Clog P \text{ vs } MR_{-3Ph} = 0.286 \end{aligned} \quad (49)$$

$$\begin{aligned} \log(1/IC_{50}) &= 0.135(\pm 0.033) MR_{-3Ph} + 7.051(\pm 0.116) \\ n &= 15, r = 0.924, r^2 = 0.855, q^2 = 0.805, s = 0.141, Q = 6.553, \\ F_{1,13} &= 76.488, \alpha = 0.01 \end{aligned} \quad (50)$$

3 Conclusion

All the above QSAR studies on hydroxamic acids acting as HDAC inhibitors have shown the importance of basically two properties of the compounds, the hydrophobicity and molar refractivity, where in the majority of cases the latter has been more dominant. They basically indicate the involvement of dispersion, or say,

essentially the electrostatic interaction with the receptor. In a few cases, there can be, however, the hydrophobic interaction, too. In a few cases, the negative coefficient of MR also suggests the steric effect of bulky substituent or of the whole molecule. All the three kinds of interactions, i.e., electrostatic, hydrophobic, and steric have also been demonstrated by CoMFA and CoMSIA studies performed on several cases. Thus all the studies have provided the guidelines for designing better, more potent HDAC inhibitors in the class of hydroxamic acids.

References

- Angibaud P, Arts J, Van Emelen K et al (2005) Discovery of pyrimidyl-5-hydroxamic acids as new potent histone deacetylase inhibitors. *Eur J Med Chem* 40:597–606
- Belvedere S, Witter DJ, Yan J et al (2007) Aminosuberoyl hydroxamic acids (ASHAs): a potent new class of HDAC inhibitors. *Bioorg Med Chem Lett* 17:3969–3971
- Bieliauskas AV, Weerasinghe SVW, Pflum MKH (2007) Structural requirements of HDAC inhibitors: SAHA analogs functionalized adjacent to the hydroxamic acid. *Bioorg Med Chem Lett* 17:2216–2219
- Bouchain G, Leit S, Frechette S et al (2003) Development of potential antitumor agents. Synthesis and biological evaluation of a new set of sulfonamide derivatives as histone deacetylase inhibitors. *J Med Chem* 46:820–830
- Charrier C, Bertrand P, Gesson JP et al (2006) Synthesis of rigid trichostatin A analogs as HDAC inhibitors. *Bioorg Med Chem Lett* 16:5339–5344
- Chen Y, Jiang YJ, Zhou JW et al (2008a) Identification of ligand features essential for HDACs inhibitors by pharmacophore modeling. *J Mol Graph Model* 26:1160–1168
- Chen Y, Li H, Tang W et al (2009) 3D-QSAR studies of HDACs inhibitors using pharmacophore-based alignment. *Eur J Med Chem* 44:2868–2876
- Chen Y, Lopez-Sanchez M, Savoy DN et al (2008b) A series of potent and selective, triazolylphenyl-based histone deacetylases inhibitors with activity against pancreatic cancer cells and *Plasmodium falciparum*. *J Med Chem* 51:3437–3448
- Curtin ML, Garland RB, Heyman HR et al (2002) Succinimide hydroxamic acids as potent inhibitors of histone deacetylase (HDAC). *Bioorg Med Chem Lett* 12:2919–2923
- Dai Y, Guo Y, Guo J et al (2003) Indole amide hydroxamic acids as potent inhibitors of histone deacetylases. *Bioorg Med Chem Lett* 13:1897–1901
- Dawson M, Xia Z, Liu G et al (2007) An adamantyl-substituted retinoid-derived molecule that inhibits cancer cell growth and angiogenesis by inducing apoptosis and binds to small heterodimer partner nuclear receptor: effects of modifying its carboxylate group on apoptosis, proliferation, and protein-tyrosine phosphatase activity. *J Med Chem* 50:2622–2639
- Delorme D, Ruel R, Lavoie R et al (2001) Inhibitors of histone deacetylase, methylgene, Inc Int Patent Appl WO 01/38322
- Dessalew N (2007) QSAR study on aminophenylbenzamides and acrylamides as histone deacetylase inhibitors: an insight into the structural basis of antiproliferative activity. *Med Chem Res* 16:449–460
- Domingo JL (1998) Developmental toxicity of metal chelating agents. *Reprod Toxicol* 12:499–510
- El Yazal J, Pang YP (2000) Proton dissociation energies of zinc-coordinated hydroxamic acids and their relative affinities for zinc: insight into design of inhibitors of zinc-containing proteinases. *J Phys Chem B* 104:6499–6504
- Green ES, Evans H, Rice-Evans P et al (1993) The efficacy of monohydroxamates as free radical scavenging agents compared with di- and trihydroxamates. *Biochem Pharmacol* 45:357–366

- Guo Y, Xiao J, Guo Z et al (2005) Exploration of a binding mode of indole amide analogues as potent histone deacetylase inhibitors and 3D-QSAR analyses. *Bioorg Med Chem Lett* 13:5424–5434
- Gupta SP (2011) *QSAR and molecular modeling*. Anamaya, New Delhi
- Jaiswal D, Karthikeyan C, Shrivastava SK et al (2006) QSAR modeling of sulfonamide inhibitors of histone deacetylase. *Int Electr J Mol Des* 5:345–354
- Jung M, Brosch G, Kolle D et al (1999) Amide analogues of trichostatin A as inhibitors of histone deacetylase and inducers of terminal cell differentiation. *J Med Chem* 42:4669–4679
- Juvale DC, Kulkarni VV, Deokar HH et al (2006) 3D-QSAR of histone deacetylase inhibitors: hydroxamate analogues. *Org Biomol Chem* 4:2858–2868
- Katritzky AR, Slavov SH, Dobchev DA et al (2007) Comparison between 2D and 3D-QSAR approaches to correlate inhibitor activity for a series of indole amide hydroxamic acids. *QSAR Comb Sci* 3:333–345
- Kim DK, Lee JY, Kim JS et al (2003) Synthesis and biological evaluation of 3-(4-substituted-phenyl)-*N*-hydroxy-2-propenamides, a new class of histone deacetylase inhibitors. *J Med Chem* 46:5745–5751
- Kim HM, Ryu DK, Choi Y et al (2007) Structure-activity relationship studies of a series of novel delta-lactam-based histone deacetylase inhibitors. *J Med Chem* 50:2737–2741
- Kozikowski AP, Chen Y, Gaysin AM et al (2008) Chemistry, biology, and QSAR studies of substituted biaryl hydroxamates and mercaptoacetamides as HDAC inhibitors-nanomolar-potency inhibitors of pancreatic cancer cell growth. *Chem Med Chem* 3:487–501
- Lavoie R, Bouchain G, Frechette S et al (2001) Design and synthesis of a novel class of histone deacetylase inhibitors. *Bioorg Med Chem Lett* 11:2847–2850
- Lipczynska-Kochany E (1988) In: Some new aspects of hydroxamic acid chemistry. *E. Pr Nauk Politech Warsz Chem* 46:3–98
- Liu B, Lu AJ, Liao CZ et al (2005) 3D-QSAR of sulfonamide hydroxamic acid HDAC inhibitors. *Acta Phys Chim Sin* 21:333–337
- Lu Q, Wang DS, Chen CS et al (2005) Structure-based optimization of phenylbutyrate-derived histone deacetylase inhibitors. *J Med Chem* 48:5530–5535
- Mahboobi S, Sellmer A, Höcher H et al (2007) 2-aryloindoles and 2-aryloxybenzofurans with *N*-hydroxyacrylamide substructures as a novel series of rationally designed histone deacetylase inhibitors. *J Med Chem* 50:4405–4418
- Mai A, Massa S, Cerbara I et al (2004) 3-(4-Aroyl-1-methyl-1*H*-2-pyrrolyl)-*N*-hydroxy-2-propenamides as a new class of synthetic histone deacetylase inhibitors. 2. Effect of pyrrole-C2 and/or -C4 substitutions on biological activity. *J Med Chem* 47:1098–1109
- Mai A, Massa S, Pezzi R et al (2003a) Discovery of (aryloxopropenyl)pyrrolyl hydroxyamides as selective inhibitors of class IIa histone deacetylase homologue HD1-A. *J Med Chem* 46:4826–4829
- Mai A, Massa S, Pezzi R et al (2005a) Class II (IIa)-selective histone deacetylase inhibitors. 1. Synthesis and biological evaluation of novel (aryloxopropenyl)pyrrolyl hydroxyamides. *J Med Chem* 48:3344–3353
- Mai A, Massa S, Ragno R et al (2002) Binding mode analysis of 3-(4-benzoyl-1-methyl-1*H*-2-pyrrolyl)-*N*-hydroxy-2-propenamide: a new synthetic histone deacetylase inhibitor inducing histone hyperacetylation, growth inhibition, and terminal cell differentiation. *J Med Chem* 45:1778–1784
- Mai A, Massa S, Ragno R et al (2003b) 3-(4 Aroyl-1-methyl-1*H*-2-pyrrolyl)-*N*-hydroxy-2-alkylamides as a new class of synthetic histone deacetylase inhibitors. 1. Design, synthesis, biological evaluation, and binding mode studies performed through three different docking procedures. *J Med Chem* 46:512–524
- Mai A, Massa S, Rotili D et al (2005b) Exploring the connection unit in the HDAC inhibitor pharmacophore model: novel uracil-based hydroxamates. *Bioorg Med Chem Lett* 15:4656–4661
- Massa S, Mai A, Sbardella G et al (2001) 3-(4-aryloxy-1*H*-pyrrol-2-yl)-*N*-hydroxy-2-propenamides, a new class of synthetic histone deacetylase inhibitors. *J Med Chem* 44:2069–2072

- Melagraki G, Afantitis A, Sarimveis H et al (2009) Predictive QSAR workflow for the in silico identification and screening of novel HDAC inhibitors. *Mol Divers* 13:301–311
- Moradei O, Leit S, Zhou N et al (2006) Substituted *N*-(2-aminophenyl)-benzamides, (*E*)-*N*-(2-aminophenyl)-acrylamides and their analogues: novel classes of histone deacetylase inhibitors. *Bioorg Med Chem Lett* 16:4048–4052
- Munster PN, Troso-Sandoval T, Rosen N et al (2001) The histone deacetylase inhibitor suberoylanilide hydroxamic acid induces differentiation of human breast cancer cells. *Cancer Res* 61:8492–8497
- Muri EMF, Nieto MJ, Sindelar RD et al (2002) Hydroxamic acids as pharmacological agents. *Cur Med Chem* 9:1631–1653
- Nagaoka Y, Maeda T, Kawai Y et al (2006) Synthesis and cancer antiproliferative activity of new histone deacetylase inhibitors: hydrophilic hydroxamates and 2-aminobenzamide containing derivatives. *Eur J Med Chem* 41:697–708
- Niemeyer HM, Pesel E, Copaja SV et al (1989) Changes in hydroxamic acid levels of wheat plants induced by aphid feeding. *Phytochem* 28:447–449
- Park H, Lee S (2004) Homology modeling, force field design, and free energy simulation studies to optimize the activities of histone deacetylase inhibitors. *J Comp-Aid Mol Des* 18:375–388
- Parvathy S, Hussain I, Karran EH et al (1998) Alzheimer's amyloid precursor protein alpha-secretase is inhibited by hydroxamic acid-based zinc metalloprotease inhibitors: similarities to the angiotensin converting enzyme secretase. *Biochem* 37:1680–1685
- Pontiki E, Hadjipavlou- Litina D, Geromichalos G et al (2009) Anticancer activity and quantitative–structure activity relationship (QSAR) studies of a series of antioxidant/anti-inflammatory aryl-Acetic and hydroxamic Acids. *Chem Biol Drug Des* 74:266–275
- Pontiki E, Hadjipavlou-Litina D (2012) Histone deacetylase inhibitors (HDACIs). Structure-activity relationships: history and new QSAR perspectives. *Med Res Rev* 32:1–165
- Price S, Bordogna W, Braganza R et al (2007a) Identification and optimisation of a series of substituted 5-pyridin-2-yl-thiophene-2-hydroxamic acids as potent histone deacetylase (HDAC) inhibitors. *Bioorg Med Chem Lett* 17:363–369
- Price S, Bordogna W, Bull RJ et al (2007b) Identification and optimisation of a series of substituted 5-(1*H*-pyrazol-3-yl) thiophene-2-hydroxamic acids as potent histone deacetylase (HDAC) inhibitors. *Bioorg Med Chem Lett* 17:370–375
- Ragno R, Simeoni S, Rotili D et al (2008) Class II-selective histone deacetylase inhibitors. Part 2: alignment-independent GRIND 3-D QSAR, homology and docking studies. *Eur J Med Chem* 43:621–632
- Ragno R, Simeoni S, Valente S et al (2006) 3-D QSAR studies on histone deacetylase inhibitors. A GOLPE/GRID approach on different series of compounds. *J Chem Inf Model* 46:1420–1430
- Rajwade RP, Pande R, Mishra KP et al (2009) Hydroxamic acids analogous against breast cancer cells: 2D-QSAR and 3D-QSAR studies. *QSAR Comb Sci* 28:1500–1508
- Rajwade RP, Pande R, Mishra KP et al (2008) Quantitative structure—activity relationship (QSAR) of *N*-arylsubstituted hydroxamic acids as inhibitors of human adenocarcinoma cells A431. *Med Chem* 4:237–243
- Remiszewski SW, Sambucetti LC, Atadja P et al (2002) Inhibitors of human histone deacetylase: synthesis and enzyme and cellular activity of straight chain hydroxamates. *J Med Chem* 45:753–757
- Remiszewski SW, Sambucetti LC, Bair KW et al (2003) *N*-hydroxy-3-phenyl-2-propenamides as novel inhibitors of human histone deacetylase with in vivo antitumor activity: discovery of (2*E*)-*N*-hydroxy-3-[4-[(2-hydroxyethyl) [2-(1*H*-indol-3-yl) ethyl] amino] methyl]phenyl]-2-propenamide (NVP-LAQ824). *J Med Chem* 46:4609–4624
- Shinji C, Maeda S, Imai K et al (2006) Design, synthesis, and evaluation of cyclic amide/imide-bearing hydroxamic acid derivatives as class-selective histone deacetylase (HDAC) inhibitors. *Bioorg Med Chem* 14:7625–7651
- Shinji C, Nakamura T, Maeda S et al (2005) Design and synthesis of phthalimide-type histone deacetylase inhibitors. *Bioorg Med Chem Lett* 15:4427–4431

- Silverman RB (2004) *The organic chemistry of drug design and drug action*. Academic Press, USA
- Steward WP, Thomas AL (2000) Marimastat: the clinical development of a matrix metalloproteinase inhibitor. *Expert Opin Invest Drugs* 9:2913–2922
- Taira J, Chika M, Aniya Y (2002) Dimerumic acid as an antioxidant from the mold, *Monascus anka*: the inhibition mechanisms against lipid peroxidation and heme protein-mediated oxidation. *Biochem Pharmacol* 63:1019–1026
- Turcot I, Stintzi A, Xu J et al (2000) Fast biological iron chelators: kinetics of iron removal from human ferric transferrin by multidentate hydroxypyridonates. *Biol Inorg Chem* 5:634–641
- Vadivelan S, Sinha BN, Rambabu G et al (2008) Pharmacophore modeling and virtual screening studies to design some potential histone deacetylase inhibitors as new leads. *J Mol Graph Model* 26:935–946
- Wagh NK, Deokar HS, Juvele DC et al (2006) 3D-QSAR of histone deacetylase inhibitors as anticancer agents by genetic function approximation. *Ind J Biochem Biophys* 43:360–371
- Wang DF, Wiest O, Helquist P et al (2004) QSAR studies of PC-3 cell line inhibition activity of TSA and SAHA-like hydroxamic acids. *Bioorg Med Chem Lett* 14:707–711
- Wittich S, Scherf H, Xie C et al (2002) Structure-activity relationships on phenylalanine-containing inhibitors of histone deacetylase: in vitro enzyme inhibition, induction of differentiation, and inhibition of proliferation in Friend leukemic cells. *J Med Chem* 45:3296–3309
- Woo SH, Frechette S, Abou Khalil E et al (2002) Structurally simple trichostatin A-like straight chain hydroxamates as potent histone deacetylase inhibitors. *J Med Chem* 45:2877–2885
- Xie A, Liao C, Li Z et al (2004) Quantitative structure-activity relationship study of histone deacetylase inhibitors. *Curr Med Chem Anticancer Agents* 4:273–299
- Zhang L, Fang H, Zhu HW et al (2009) QSAR studies of histone deacetylase (HDAC) inhibitors by CoMFA, CoMSIA, and molecular docking. *Drug Discov Ther* 3:41–48